Rapid Communications

Bidirectional switching assisted by interlayer exchange coupling in asymmetric magnetic tunnel junctions

D. J. P. de Sousa,[1,*] P. M. Haney,[2] D. L. Zhang,[1] J. P. Wang,[1,†] and Tony Low[1,‡]
[1]*Department of Electrical and Computer Engineering, University of Minnesota, Minneapolis, Minnesota 55455, USA*
[2]*Physical Measurement Laboratory, National Institute of Standards and Technology, Gaithersburg, Maryland 20899-6202, USA*

(Received 17 November 2019; accepted 29 January 2020; published 11 February 2020)

We study the combined effects of spin transfer torque, voltage modulation of interlayer exchange coupling, and magnetic anisotropy on the switching behavior of perpendicular magnetic tunnel junctions (p-MTJs). In asymmetric p-MTJs, a linear-in-voltage dependence of interlayer exchange coupling enables the effective perpendicular anisotropy barrier to be lowered for both voltage polarities. This mechanism is shown to reduce the critical switching current and effective activation energy. Finally, we analyze the possibility of having switching via interlayer exchange coupling only.

DOI: 10.1103/PhysRevB.101.081404

Introduction. Magnetic tunnel junctions (MTJs) that can be switched bidirectionally by electrical means are highly desirable for low-power consumption applications [1]. Current-induced magnetization reversal is one of the most promising and reliable technologies available for achieving bidirectional switching in MTJs [2–5].

Current-induced switching relies on spin transfer torque (STT), where the interaction between current-carrying spins which are misaligned with the magnetization leads to magnetic dynamics and reversal [4]. In addition to STT, a charge current modifies the interlayer exchange coupling (IEC) between fixed and free layers via an additional fieldlike torque [5–7]. Though frequently called "fieldlike spin transfer torque component," in this work we refer to this torque component as interlayer exchange torque [6]. Denoting the free (pinned) magnetic layer orientation by $\mathbf{m}$ ($\mathbf{m}_p$) [see inset in Fig. 1(a)], the total current-induced torque density is

$$\mathcal{N} = T_{\mathrm{IEC}}\mathbf{m}\times\mathbf{m}_p + T_{\mathrm{STT}}\mathbf{m}\times(\mathbf{m}\times\mathbf{m}_p). \tag{1}$$

Unlike in spin valves where the IEC torque is negligible, it has been demonstrated that T_{IEC} is comparable to T_{STT} in MgO-based MTJs, considerably affecting the magnetization dynamics of the free layer [8–10]. However, while the importance of T_{STT} for magnetization switching is well understood, the contribution of T_{IEC} is often omitted in many analyses and poorly explored.

For perpendicular MTJs (p-MTJs), the critical switching current J_c is directly proportional to the total effective perpendicular anisotropy K_{eff} [11,12]. Such proportionality reflects the fundamental problem encountered in memory technology, where one seeks to improve K_{eff} for better retention of information while reducing the critical switching current J_c for low-power consumption [12]. Particularly, the voltage control of magnetic anisotropy (VCMA) is currently being quoted as one of the most promising methods to circumvent this problem, as it provides a mechanism to reduce the anisotropy barrier $K_{\mathrm{eff}}\mathcal{V}$, where $\mathcal{V}$ is the volume of the free layer, only when a voltage is applied across the MTJ, enabling one to reduce J_c momentarily while maintaining a sizable K_{eff} at zero applied voltage [12–15]. However, while it can reduce the critical switching current for a given applied voltage by reducing K_{eff}, it tends to increase K_{eff} for the opposite voltage polarity. The ability to overcome the anisotropy barrier bidirectionally while decreasing the critical current density is highly desirable, and remains a long-standing goal in the search for low-power consumption spintronics.

In this work, we show that T_{IEC} can assist STT switching by effectively reducing the anisotropy barrier for both voltage polarities in asymmetric p-MTJs. We demonstrate that T_{IEC} directly competes with the total effective intrinsic uniaxial anisotropy quantified by K_{eff}, enabling one to reduce the critical switching current bidirectionally by tuning the degree of asymmetry of the p-MTJ. Our model includes the combined effects of STT, VCMA and IEC effects on p-MTJs, which are all known to be present in this kind of system [12,16].

The total torque acting on the magnetization vector of the free layer is decomposed into different contributions, as given by the Landau-Lifshitz-Gilbert equation [17]

$$\frac{d\mathbf{m}}{dt} = -\gamma\mathbf{m}\times\mathbf{H}_{\mathrm{eff}} + \alpha\mathbf{m}\times\frac{d\mathbf{m}}{dt} + \frac{\gamma}{\mu_0 M_S t_{\mathrm{free}}}\mathcal{N}, \tag{2}$$

where $\mathbf{m} = \mathbf{M}/M_S$, with $\mathbf{M}$ being the magnetization of the free layer with saturation M_S, γ is the gyromagnetic ratio, α is the intrinsic damping parameter, μ_0 is the vacuum permeability, and t_{free} is the thickness of the free layer. The effective field is $\mathbf{H}_{\mathrm{eff}} = [2K_{\mathrm{eff}}(V)m_z/\mu_0 M_S]\mathbf{z}$, with $\mathbf{z}$ being the axis perpendicular to the free layer plane and m_z being the z component of $\mathbf{m}$. The total effective anisotropy coefficient is given by $K_{\mathrm{eff}}(V) = K_{\mathrm{eff}}(0) + \xi V$ with $K_{\mathrm{eff}}(0) = K_i/t_{\mathrm{free}} - \mu_0 M_S^2/2$ being the effective perpendicular magnetic anisotropy at zero voltage with interfacial anisotropy K_i. The VCMA coefficient

*sousa020@umn.edu
†jpwang@umn.edu
‡tlow@umn.edu

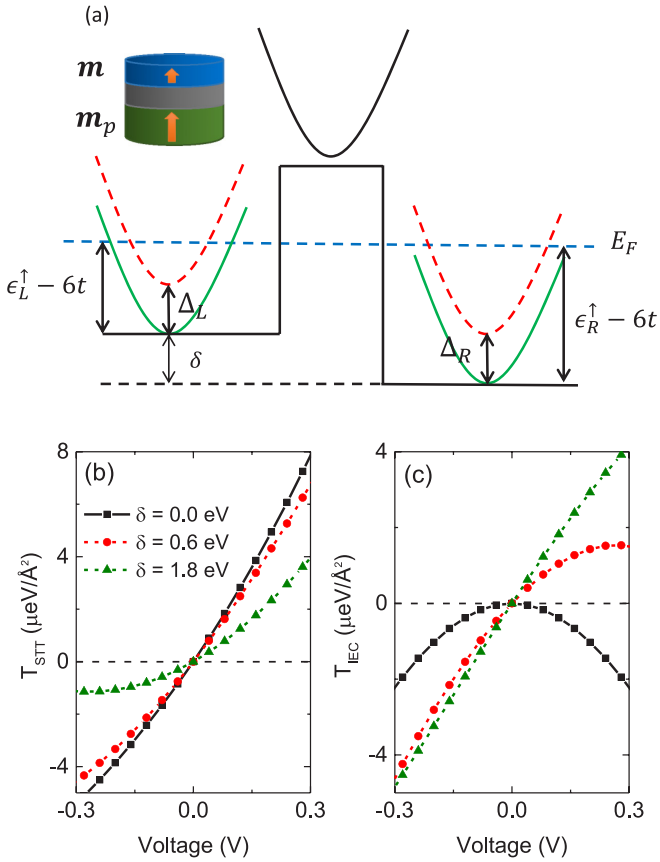

FIG. 1. (a) MTJ band diagram. The parameter $\delta = \epsilon_L^{\uparrow(\downarrow)} - \epsilon_R^{\uparrow(\downarrow)}$ controls the asymmetry of the MTJ. The bottom of the spin-up (down) bands in the single orbital tight-binding approach is $\epsilon^{\uparrow(\downarrow)} - 6t$, where t is the nearest-neighbor hopping parameter. The inset shows a sketch of an asymmetric p-MTJ with $\mathbf{m}$ and $\mathbf{m}_p$ corresponding to the unit vectors in the direction of the magnetization of the free and fixed layer, respectively. Panels (b) and (c) show the voltage dependence of spin transfer torque and nonequilibrium interlayer exchange coupling, respectively, for different MTJ asymmetries δ, as defined in (a).

is ξ and V the applied voltage across the p-MTJ. We assume $\mathbf{m}_p = \mathbf{z}$, i.e., perpendicular to the interface.

The critical switching voltage V_c is given by the following implicit equation [18]:

$$T_{\rm STT}(V_c) = 2\alpha t_{\rm free}\left[K_{\rm eff}(V_c)m_z - \tfrac{T_{\rm IEC}(V_c)}{2t_{\rm free}}\right], \tag{3}$$

where $m_z = \pm 1$ for magnetization initially in the parallel (P, with $m_z = +1$) or antiparallel (AP, with $m_z = -1$) configuration. This result reveals that while $T_{\rm STT}$ acts in favor or against the intrinsic damping [4], $T_{\rm IEC}$ competes directly with the anisotropy torque, affecting the final critical STT switching magnitude $T_{\rm STT}^c = T_{\rm STT}(V_c)$. Before analyzing the consequences of this equation from the perspective of the quantum transport model, let us suppose, for simplicity, the following voltage dependencies of the torques, i.e., $T_{\rm STT} = \beta_{\rm STT}V$, $T_{\rm IEC} = C_1V + C_2V^2$, where the coefficients $\beta_{\rm STT}$, C_1, and C_2 express the voltage modulation of the nonequilibrium torques to lowest order in V. Our convention for the voltage is that $V > 0$ leads to an electron flow from the fixed layer to the free layer. For symmetric p-MTJs, $T_{\rm IEC}$ is an even function of applied voltage, i.e., the spatial top-bottom symmetry requires that $C_1 = 0$ and $C_2 \neq 0$ [19]. In this case, one can solve Eq. (3) analytically for V_c to find

$$V_c = \frac{2\alpha t_{\rm free}}{\beta_{\rm STT}} K_{\rm eff}(0)m_z, \tag{4}$$

where we have assumed $\xi = 0$, i.e., no VCMA effect, and neglected terms of order α^2. Interestingly, Eq. (4) shows that V_c does not depend on C_2 in this limit. Hence, this result is consistent with the fact that $T_{\rm IEC}$ has little or no influence on the magnetization switching in conventional symmetric p-MTJs.

The situation for asymmetric p-MTJs is different. In this case, theoretical [7,20] and experimental [21] analyses have shown that $C_1 \neq 0$, giving a sizable linear voltage-dependent contribution to $T_{\rm IEC}$. In this situation, $T_{\rm IEC}$ acts like a torque due to an effective field with sign determined by V and direction aligned with the magnetization of the fixed layer. For a given applied voltage V, this results in a unidirectional anisotropy, to be contrasted with the intrinsic uniaxial magnetic anisotropy. We explore the consequences of this symmetry breaking induced contribution by assuming, for simplicity, $\xi = 0$ and $C_2 = 0$. Equation (3) can then be easily solved:

$$V_c = \frac{2\alpha t_{\rm free}}{\beta_{\rm STT}} K_{\rm eff}(0)m_z(1 + \alpha C_1/\beta_{\rm STT})^{-1}, \tag{5}$$

where V_c is reduced by a factor of $1 + \alpha C_1/\beta_{\rm STT}$. This simple analysis shows the relevance of $T_{\rm IEC}$ in reducing the critical switching current. A comparison between experiments from Refs. [8,21] indicates that $C_1 = 0$ and $C_1 \approx 30$ kA/m for symmetric and asymmetric CoFeB/MgO/CoFeB MTJs, respectively. These results show the possibility of tuning V_c via C_1.

The above analysis, albeit qualitative, demonstrates the possibility of reducing critical switching voltage when $T_{\rm IEC}$ exhibits strong asymmetric dependence on voltage, i.e., $C_1 \gg 0$. According to Eq. (5), the sign of $C_1/\beta_{\rm STT}$ must be positive in order to decrease the V_c. While $\beta_{\rm STT}$ is usually positive, it was experimentally observed that one can tune the sign and magnitude of C_1 by controlling the relative composition between fixed and free magnetic layers [21]. In the following section, we first evaluate the voltage modulation of both $T_{\rm STT}$ and $T_{\rm IEC}$ within a single orbital quantum transport model and explore the dependence of the critical current density with p-MTJ asymmetry.

Nonequilibrium torques. In the absence of spin-orbit coupling [22], the torque exerted on the magnetization of the ith atomic plane of the free layer is related to the spin-current flux into that plane as $\mathbf{T}_i = -\nabla \cdot \mathbf{Q}_i = \mathbf{Q}_{i-1,i} - \mathbf{Q}_{i,i+1}$ where $\mathbf{Q}_{i,j}$ is the spin-current density between atomic planes i and j. The total torque exerted on the semi-infinite magnetic lead reads $\mathbf{T} = \sum_i \mathbf{T}_i = \mathbf{Q}_{\rm Ox/FM}$, where $\mathbf{Q}_{\rm Ox/FM}$ is the spin-current density penetrating the magnetic lead at the oxide-ferromagnet interface [7,20]. Assuming a spin quantization axis along the $\mathbf{m}_p = \mathbf{z}$ direction for the fixed layer, the $T_{\rm STT}$ and $T_{\rm IEC}$ components are obtained by extracting the $\mathbf{m} \times (\mathbf{m} \times \mathbf{m}_p)$ and $\mathbf{m} \times \mathbf{m}_p$ components, respectively, of the interface spin current $\mathbf{Q}_{\rm Ox/FM}$ [7,19,20].

We employ the single-orbital tight-binding model and express the spin-current density as [7,19,20]

$$\mathbf{Q}_{i,j} = \frac{1}{4\pi}\int_{\Omega_B}\frac{d^2\mathbf{k}_\parallel}{(2\pi)^2}\int dE\ \mathrm{Tr}_\sigma[(H_{ji}G^<_{ij} - H_{ij}G^<_{ji})\vec{\sigma}], \quad (6)$$

where $\vec{\sigma} = (\sigma_x, \sigma_y, \sigma_z)$ is the vector of Pauli matrices, H_{ij} is the hopping matrix between sites i and j, $G^<_{ij}$ is the lesser Green's function of the whole coupled system, and the $\mathbf{k}_\parallel$ integration is performed over the two-dimensional in-plane Brillouin zone Ω_B. This model provides an accurate description of the voltage dependence of the nonequilibrium torques in systems such as in Fe/MgO/Fe MTJs [23–26].

In experiments, asymmetry in the ferromagnetic contacts can be introduced through the use of different metals [27], or by considering ferromagnets with different compositions such as in $Co_{40}Fe_{40}B_{20}/MgO/Co_{49}Fe_{21}B_{20}$ MTJs [21]. In this work, we introduce asymmetry in the ferromagnets by adjusting their band fillings. The symmetry breaking is controlled by the asymmetry parameter $\delta = \epsilon_R^{\uparrow(\downarrow)} - \epsilon_L^{\uparrow(\downarrow)}$, where $\epsilon_{L(R)}^{\uparrow(\downarrow)}$ refers to the spin-up (down) band filling of the left (right) magnetic lead, as shown by the band diagram in Fig. 1(a). The exchange splitting inside the ferromagnets are kept constant and the same, i.e., $\Delta_L = \Delta_R$.

The voltage dependence of T_{STT} and T_{IEC} for different asymmetries [$\delta = 0.0$ eV (solid black), $\delta = 0.6$ eV (dashed red), and $\delta = 1.8$ eV (dot-dashed olive)] are shown in Figs. 1(b) and 1(c), respectively. The angular dependencies of both torque components are $\sin(\theta)$. Hence, it suffices to show only their amplitudes. The results of Fig. 1(b) show that T_{STT} presents an approximately linear behavior for small applied voltages, i.e., $T_{\mathrm{STT}} \approx \beta_{\mathrm{STT}} V$, with a slope that decreases as an increasing function of the asymmetry parameter δ. In particular, for the most asymmetric case considered ($\delta = 1.8$ eV), the voltage behavior of T_{STT} at negative V deviates from linear and one can potentially achieve T_{STT} sign reversal under applied voltages for one of the polarities [19]. Figure 1(c) indicates that T_{IEC} is quadratic in V for symmetric p-MTJs, i.e., $T_{\mathrm{IEC}} \approx C_2 V^2$ with $C_2 < 0$, as theoretically predicted and observed experimentally [4,7,8,20]. As one increases the asymmetry via δ, the voltage modulation of T_{IEC} is enhanced while an additional linear-in-voltage contribution develops, i.e., $T_{\mathrm{IEC}} \approx C_1 V + O(V^2)$. We also emphasize that the ratio C_1/β_{STT} is positive if one chooses $\delta > 0$.

Critical current density. The critical current density J_c is computed by computing the current-voltage relation using Landauer's formula and nonequilibrium Green's function. This relation enables the previously computed voltage-dependent T_{IEC} and T_{SST} to be converted to their corresponding current dependent. Figure 2(a) shows J_c as a function of the asymmetry parameter δ for P to AP (red circles) and AP to P (blue triangles) switching with $K_i \approx 1.3$ mJ/m^2, and VCMA coefficient $\xi = 20$ kJ/V m^3. The result clearly shows that J_c decreases with asymmetry, which can be interpreted as follows: The presence of T_{IEC} in asymmetric p-MTJs reduces K_{eff} for both voltage polarities, as qualitatively described by Eq. (5). Therefore, the effective energy barrier between P and AP configurations decreases and less current is necessary for magnetization reversal.

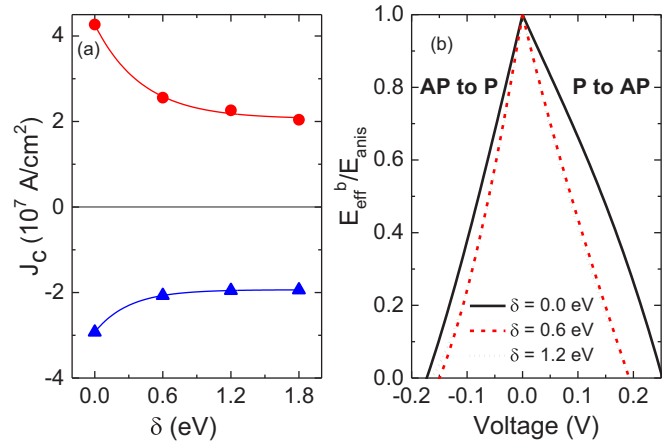

FIG. 2. Critical current density as a function of the asymmetry parameter δ. The red circles (blue triangles) show the trend for P to AP (AP to P) switching. (b) Normalized effective activation energy as a function of applied voltage for different p-MTJ asymmetries for P to AP ($V > 0$) and AP to P ($V < 0$) switching.

The symmetry breaking also has important consequences for thermally activated switching. Following Ref. [28], we have derived expressions for the effective activation energy in the presence of T_{IEC}:

$$E^b_{\mathrm{eff}} = E_{\mathrm{anis}}\left(1 - \frac{T_{\mathrm{STT}}}{T^c_{\mathrm{STT}}}\right)\left(1 - m_z\frac{T_{\mathrm{IEC}}}{2t_{\mathrm{free}}K_{\mathrm{eff}}}\right), \quad (7)$$

from which one can extract the switching time $\tau^{-1} = f_0 \exp(-E^b_{\mathrm{eff}}/k_BT)$, with f_0 being an attempt frequency. The anisotropy energy barrier $E_{\mathrm{anis}}(V) = K_{\mathrm{eff}}(V)\mathcal{V}$ quantifies the thermal stability factor $\Delta = E_{\mathrm{anis}}(0)/k_BT$. Figure 2(b) shows the voltage dependence of the normalized effective energy barrier $E^b_{\mathrm{eff}}/E_{\mathrm{anis}}$ for P to AP ($V > 0$) and AP to P ($V < 0$) switching considering several different asymmetry parameters δ. In this plot we use the voltage dependence of nonequilibrium torques from the quantum transport model. As one can see, the activation energy drops faster with V for asymmetric p-MTJs, allowing for higher switching probabilities at a given temperature T.

Switching by voltage control of IEC. So far, we have shown that in asymmetric p-MTJ, T_{IEC} can assist STT switching by effectively reducing the anisotropy barrier for both voltage polarities. Anisotropy and voltage-dependent IEC torques can be written as derivatives of an effective energy, given by

$$E(\theta) = K_{\mathrm{eff}}\sin(\theta)^2 + (T_{\mathrm{IEC}}/t_{\mathrm{free}})\cos(\theta), \quad (8)$$

where θ is the angle between $\mathbf{m}$ and $\mathbf{m}_p$. Stable equilibrium points are found at energy minima, where the total fieldlike torque vanishes.

Figures 3(a) and 3(b) show the energy landscape for negative and positive current density of $J = 5 \times 10^7$ A/cm^2 for different p-MTJ asymmetries. We have also plotted the energy at zero applied voltage in black solid lines for comparison purposes. One sees that K_{eff} alone gives rise to two metastable equilibrium configurations with P ($\theta = 0$) or AP ($\theta = \pi$) alignment, emphasizing the axial nature of perpendicular anisotropy.

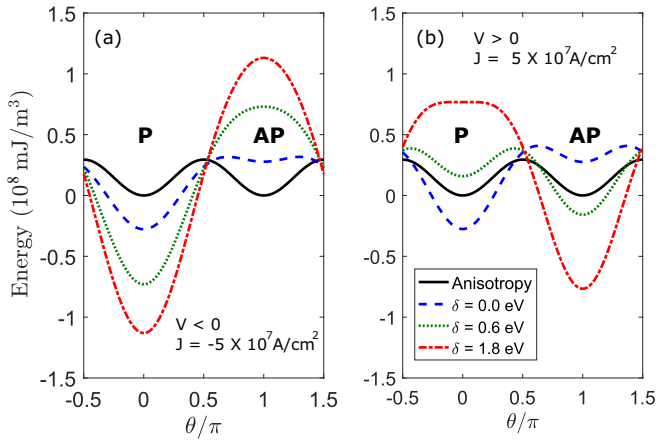

FIG. 3. Energy landscapes for (a) negative and (b) positive current densities of absolute value 5×10^7 A/cm^2 for different degrees of asymmetries δ. We define θ as the angle between the magnetization of free and pinned layers such that parallel and antiparallel configurations, highlighted as P and AP, are found in $\theta = 0$ and $\theta = \pi$, respectively. We considered $K_{\text{eff}}(0) = 29.5$ kJ/m^3 and $\xi = 20$ kJ/(V m^3). The solid black curve shows the contribution of perpendicular anisotropy only, whereas the other curves show the total energy landscape resulting from the sum of IEC and VCMA contributions.

Figure 3(a) shows the angular dependence of the total energy for different asymmetries δ at applied $V < 0$. For the symmetric case ($\delta = 0$ eV), a negative bias voltage gives rise to a negative T_{IEC} [see Fig. 1(c)] while decreasing K_{eff}. The associated energy landscape for this case is shown as a dashed blue curve in Fig. 3(a). One sees that the stability of the P (AP) configuration is enhanced (suppressed) due to the unidirectional nature of the IEC torque. The dotted olive curve in Fig. 3(a) shows the angular dependence of energy for the same current density considering an asymmetric p-MTJ with $\delta = 0.6$ eV. In this case, the previously metastable AP configuration is now a maximum, indicating a current-induced instability and subsequent switching from $\theta = \pi$ to $\theta = 0$. The dash-dotted red curve shows that the effect is even more pronounced if one further increases the asymmetry to $\delta = 1.8$ eV.

For $V > 0$, K_{eff} now increases with V. For symmetric p-MTJs, T_{IEC} is an even function of the bias and, therefore, remains negative with positive applied voltage [see Fig. 1(c)]. The resulting energy landscape is represented by the dashed blue curve in Fig. 3(b), where one observes an even greater stability in the P configuration, increasing the difficulty to switch from P to AP. In asymmetric p-MTJs, however, T_{IEC} changes sign under reversal of the voltage polarity. Such behavior results in the curves corresponding to $\delta \neq 0$ eV in Fig. 3(b). In these cases, the P (AP) configuration tends to become more unstable (stable) as one increases the asymmetry, favoring P to AP switching. In particular, the case $\delta = 1.8$ eV shows that one can completely destabilize the P configuration, showing pure IEC bidirectional bipolar switching.

Conclusion. We have studied the simultaneous impact of VCMA, IEC, and STT for p-MTJs. We demonstrated that for asymmetric devices, linearly varying T_{IEC} plays an important role in STT switching by renormalizing the effective anisotropy barrier. Such effect leads to reduced critical switching current for magnetization reversal, and can even lead to switching based on IEC alone.

Acknowledgments. This work was partially supported by C-SPIN/STARnet, DARPA ERI FRANC program, and ASCENT/JUMP.

[1] F. Matsukura, Y. Tokura, and H. Ohno, Nat. Nanotechnol. **10**, 209 (2015).
[2] D. C. Ralph and M. D. Stiles, J. Magn. Magn. Mater. **320**, 1190 (2008).
[3] M. D. Stiles and A. Zangwill, Phys. Rev. B **66**, 014407 (2002).
[4] J. Xiao, A. Zangwill, and M. D. Stiles, Phys. Rev. B **70**, 172405 (2004).
[5] A. Kalitsov, M. Chshiev, I. Theodonis, N. Kioussis, and W. H. Butler, Phys. Rev. B **79**, 174416 (2009).
[6] P. M. Haney, C. Heiliger, and M. D. Stiles, Phys. Rev. B **79**, 054405 (2009).
[7] Y. H. Tang, N. Kioussis, A. Kalitsov, W. H. Butler, and R. Car, Phys. Rev. Lett. **103**, 057206 (2009).
[8] H. Kubota, A. Fukushima, K. Yakushiji, T. Nagahama, S. Yuasa, K. Ando, H. Maehara, Y. Nagamine, K. Tsunekawa, D. D. Djayaprawira *et al.*, Nat. Phys. **4**, 37 (2008).
[9] J. C. Sankey, Y.-T. Cui, J. Z. Sun, J. C. Slonczewski, R. A. Buhrman, and D. C. Ralph, Nat. Phys. **4**, 67 (2008).
[10] A. M. Deac, A. Fukushima, H. Kubota, H. Maehara, Y. Suzuki, S. Yuasa, Y. Nagamine, K. Tsunekawa, D. D. Djayaprawira, and N. Watanabe, Nat. Phys. **4**, 803 (2008).
[11] J. Z. Sun, Phys. Rev. B **62**, 570 (2000).
[12] B. Dieny and M. Chshiev, Rev. Mod. Phys. **89**, 025008 (2017).
[13] T. Maruyama, Y. Shiota, T. Nozaki, K. Ohta, N. Toda, M. Mizuguchi, A. A. Tulapurkar, T. Shinjo, M. Shiraishi, S. Mizukami *et al.*, Nat. Nanotechnol. **4**, 158 (2009).
[14] Y. Shiota, T. Maruyama, T. Nozaki, T. Shinjo, M. Shiraishi, and Y. Suzuki, Appl. Phys. Express **2**, 063001 (2009).
[15] W. Kang, Y. Ran, Y. Zhang, W. Lv, and W. Zhao, IEEE Trans. Nanotechnol. **16**, 387 (2017).
[16] H. Liu, D. Bedau, J. Z. Sun, S. Mangin, E. E. Fullerton, J. A. Katine, and A. D. Kent, J. Magn. Magn. Mater. **358**, 233 (2014).
[17] J. Xiao, A. Zangwill, and M. D. Stiles, Phys. Rev. B **72**, 014446 (2005).
[18] See Supplemental Material at http://link.aps.org/supplemental/10.1103/PhysRevB.101.081404 for a detailed analysis of the Landau-Lifshitz-Gilbert equation and related derivations.
[19] I. Theodonis, N. Kioussis, A. Kalitsov, M. Chshiev, and W. Butler, Phys. Rev. Lett. **97**, 237205 (2006).
[20] Y. H. Tang, N. Kioussis, A. Kalitsov, W. H. Butler, and R. Car, Phys. Rev. B **81**, 054437 (2010).
[21] S.-C. Oh, S.-Y. Park, A. Manchon, M. Chshiev, J.-H. Han, H.-W. Lee, J.-E. Lee, K.-T. Nam, Y. Jo, Y.-C. Kong, B. Dieny *et al.*, Nat. Phys. **5**, 898 (2009).

[22] P. M. Haney and M. D. Stiles, Phys. Rev. Lett. **105**, 126602 (2010).
[23] H. X. Yang, M. Chshiev, A. Kalitsov, A. Schuhl, and W. H. Butler, Appl. Phys. Lett. **96**, 262509 (2010).
[24] A. Kalitsov, P.-J. Zermatten, F. Bonell, G. Gaudin, S. Andrieu, C. Tiusan, M. Chshiev, and J. P. Velev, J. Phys.: Condens. Matter **25**, 496005 (2013).
[25] A. Kalitsov, W. Silvestre, M. Chshiev, and J. P. Velev, Phys. Rev. B **88**, 104430 (2013).
[26] M. Chsiev, I. Theodonis, A. Kalitsov, N. Kioussis, and W. H. Butler, IEEE Trans. Magn. **11**, 2543 (2008).
[27] C. W. Miller, I. K. Schuller, R. W. Dave, J. M. Slaughter, Y. Zhou, and J. Akerman, J. Appl. Phys. **103**, 07A904 (2008).
[28] Z. Li and S. Zhang, Phys. Rev. B **69**, 134416 (2004).